First-principles study on the magnetic anisotropy in multiferroic $PbVO_3$ and $BiCoO_3$

Yoshitaka URATANI[1], Tatsuya SHISHIDOU[1] and Tamio OGUCHI[1,2]

[1]*Department of Quantum Matter, ADSM, Hiroshima University, Higashihiroshima, Hiroshima 739-8530*

and

[2]*Institute for Advanced Materials Research, Hiroshima University, Higashihiroshima, Hiroshima 739-8530*

Magnetic anisotropy energies (MAE) of multiferroic $PbVO_3$ and $BiCoO_3$ are evaluated from first-principles density functional calculations. Even though both oxides have similar crystal and electronic structures, calculated easy axes of spin are different: [110] in $PbVO_3$ and [001] in $BiCoO_3$. To explain the difference, the origin of MAE is discussed with a perturbation theory by taking into account of the electronic structure obtained by the first-principles calculations.

KEYWORDS: electronic structure, first-principles calculations, spin-orbit interaction, magnetic anisotropy, multiferroics, orbital order, perovskites

1. Introduction

Multiferroic systems have more than one ferro or antiferro orderings associated with electronic and lattice degrees of freedom simultaneously. Among them, ferroelectric and ferromagnetic multiferroic systems have recently attracted much attention because of the possible existence of a magnetoelectric effect and their application to the next-generation devices.[1–4] In this context, magnetic and electric controls with the orbital degree of freedom are also an interesting topic.[5]

$BiMnO_3$ has been believed to be a rare example of the ferromagnetic and ferroelectric multiferroic systems.[6–11] In $BiMnO_3$, a ferromagnetic ordering is realized with an antiferro-orbital ordering while hybridization between Bi-6p and O-2p orbitals may lead to ferroelectricity.[12,13] However, recent first-principles and experimental results for $BiMnO_3$ have shown the most stable crystal structure with non-polar (antiferroelectric) symmetry.[14,15] $BiFeO_3$ is a ferroelectric and antiferromagnetic multiferroic oxide. When synthesized as a thin film, $BiFeO_3$ shows gigantic electric polarization and has drawn considerable attention as a lead-free substitution for $PbZr_{1-x}Ti_xO_3$ in the ferroelectric devices.[16] Related perovskite-type compounds AMO_3 (A=Bi, Pb; M=transition-metal ion) are, thus, believed to form a target area to be explored in multiferroic materials research.

Recently, $PbVO_3$ and $BiCoO_3$ have been synthesized in a bulk form by a high-pressure

and high-temperature technique and epitaxially grown in a thin-film form with pulse laser deposition.[17–23] The crystal structure of $PbVO_3$ and $BiCoO_3$ has been determined by the Rietveld technique and dc resistivity and magnetic susceptibilities have been measured.[17–19] It is found that both oxides have several similar features such as large tetragonal lattice distortion, sizable off-centered atomic displacements, semiconducting behavior and C-type antiferromagnetic ordering. These properties have been reasonably explained by our previous first-principles calculations.[24] Their ferroelectric instability mainly arises from hybridization between Pb(Bi)-6p and O-2p orbitals, being coupled with the unusual structural properties. The most interesting feature in the electronic structure is that only V(Co)-3d_{xy} band is occupied in the majority (minority) spin bands of $PbVO_3$ ($BiCoO_3$), leading to an insulating state with a formal ionic configuration of V^{4+} (d^1) (Co^{3+} (d^6)). With this electronic configuration, a stable C or G-type antiferromagnetic spin ordering can be interpreted in terms of the super-exchange interaction between the neighboring transition-metal xy orbitals mediated via O-2$p\pi$. Our results have been also confirmed by the other first-principles studies.[25–27] The basic framework of the observed crystal structure is of perovskite-type, as the same as that in the typical ferroelectric oxide $PbTiO_3$. However, the crystal structure shows quite large tetragonality (c/a ratio) of 1.229 for $PbVO_3$ and 1.267 for $BiCoO_3$, compared with 1.06 for $PbTiO_3$. Furthermore, V (Co) ion is located at a remarkably off-centered position of the O_6 octahedron, being regarded as O_5 pyramid structure. Due to such large displacements, gigantic electric polarization beyond $PbTiO_3$ can be expected. Actually our first-principles calculations with the Berry-phase method[28] predict the electric polarization of 152 $\mu C/cm^2$ for $PbVO_3$ and 179 $\mu C/cm^2$ for $BiCoO_3$.[24]

Quite recently, a neutron diffraction experiment[19] has been performed to study the magnetic properties of $BiCoO_3$ and the magnetic easy axis is found to be [001]. However, no study has been reported so far concerning the microscopic origin of the magnetic anisotropy and its relation to the crystal structure with large tetragonality and displacements.

In this paper, we investigate the magnetic anisotropy of $PbVO_3$ and $BiCoO_3$ from first-principles calculations. In order to clarify the effects of the unique electronic structure associated with the peculiar crystal structure on the magnetic anisotropy, we adopt a perturbation theory with use of the first-principles electronic structure.

2. Calculation Methods

We employ a first-principles approach based on the density functional theory (DFT) within the local spin density approximation (LSDA).[29,30] One-electron Kohn-Sham equations are solved self-consistently by using the all-electron full-potential linear augmented plane wave (FLAPW) method in a scalar-relativistic manner.[31–34] The spin-orbit interaction (SOI) is treated as the second variation after the final step of self-consistent cycle and the magnetic anisotropy energy (MAE) is evaluated by using the force theorem.[35–39] Our implementation of

the all-electron FLAPW method has been used successfully for a variety of condensed matter systems including magnetic and ferroelectric materials as well as multiferroics.[40–45] Brillouin zone (BZ) integration is performed with the tetrahedron method[46] up to $6 \times 6 \times 6$ **k**-mesh points. Since both oxide systems studied are insulating within LSDA and MAE is evaluated as an energy variation by changing the orientation of spin, one can get sufficient accuracy with such k-mesh points. Muffin-tin sphere radii are set to be 1.0 Å for Pb and Bi, 0.95 Å for V and Co, 0.7 Å for O. Because of such a small muffin-tin sphere radius for V, we treat V-3p state as valence states. The plane-wave cutoff energy is set to 25 Ry for wavefunctions, and 200 Ry for charge density and potential functions. The experimental crystal structure and atomic positions are used in the present study.[24] As previously studied, the C-type antiferromagnetic (C-AFM) structure is the most stable among the ferromagnetic and several antiferromagnetic structures and thus only the C-AFM configuration is considered in this paper. The magnetic ordering is treated by using a $\sqrt{2} \times \sqrt{2} \times 1$ cell with $P4mm$ space group.

3. Electronic Structure

Since the details of electronic structure of $PbVO_3$ and $BiCoO_3$ including the mechanism of multiferroicity have been reported previously,[24–27] we briefly summarize their important aspects for the discussion of magnetic anisotropy in this section. The band structure reveals an insulating (or semiconducting) behavior with rather small energy gaps. It is known that LSDA often underestimates the energy gaps, especially in strongly-correlated electron systems. However, we believe that the size of the energy gaps affect only marginally our qualitative conclusions about the magnetic anisotropy energy made below in this paper. Bands around the energy gaps are dominated by V-3d orbitals as shown in partial density of states projected on the cubic harmonics of V-3d are shown in Fig. 3 of ref. 24. Only the majority-spin xy state is occupied, being regarded as a V^{4+} (d^1) configuration in an ionic picture. Consequently, ferro-orbital, antiferromagnetic and ferroelectric orderings coexist simultaneously in the ground state of $PbVO_3$. Note that the Cartesian coordinates are assumed along the principal axes of the non-magnetic tetragonal unit cell. As for $BiCoO_3$, quite similar electronic structure can be seen to that in $PbVO_3$, being consistent with the stability of non-centrosymmetric tetragonal structure and C- or G-type AFM configuration.[24,26] A point different from $PbVO_3$ is that, in $BiCoO_3$, the minority-spin xy state is occupied while the majority-spin states are fully occupied. Naively speaking, we may expect a similarity also in magnetic properties between $PbVO_3$ and $BiCoO_3$. However, magnetic anisotropy is completely different, as shall be discussed below.

4. Magnetic Anisotropy Energy

To evaluate MAE, one has to calculate the angle dependence of the total energy including SOI. From the prescription of MacDonald *et al.*,[36] SOI is given as

$$H_{so} = \lambda \vec{l} \cdot \vec{\sigma}(\theta, \phi) \tag{1}$$

where $\vec{l}$ and $\vec{s}$ are the orbital and spin angular momentum operators, $\vec{\sigma}$ is the 2×2 Pauli spin matrix with $\vec{s} = \vec{\sigma}/2$ and

$$\sigma_+ = \sigma_-^\dagger = \sigma_x + i\sigma_y. \tag{2}$$

λ is the SOI operator given by

$$\lambda(r) = \frac{\hbar^2}{2M^2c^2r}\frac{dV(r)}{dr}. \tag{3}$$

The spin quantization axis is defined by its polar and azimuthal angles θ and ϕ. A rotation of the axis is given by

$$\vec{l} \cdot \vec{\sigma}(\theta, \phi) = U^\dagger(\theta, \phi) \left[\vec{l} \cdot \vec{\sigma}\right] U(\theta, \phi). \tag{4}$$

where the 2×2 spin rotation matrix U is given by

$$U = \begin{pmatrix} e^{-\frac{i}{2}\phi}\cos\frac{\theta}{2} & -e^{-\frac{i}{2}\phi}\sin\frac{\theta}{2} \\ e^{\frac{i}{2}\phi}\sin\frac{\theta}{2} & e^{\frac{i}{2}\phi}\cos\frac{\theta}{2} \end{pmatrix}. \tag{5}$$

With use of U, eq. 4 is rewritten explicitly as

$$\begin{aligned} \vec{l} \cdot \vec{\sigma}(\theta, \phi) = \sigma_z &\left[l_z \cos\theta + \frac{1}{2}\sin\theta \left(l_+ e^{-i\phi} + l_- e^{i\phi} \right) \right] \\ &+ \frac{1}{2}\sigma_+ \left[-l_z \sin\theta - l_+ \sin^2\frac{\theta}{2} e^{-i\phi} + l_- \cos^2\frac{\theta}{2} e^{i\phi} \right] \\ &+ \frac{1}{2}\sigma_- \left[-l_z \sin\theta + l_+ \cos^2\frac{\theta}{2} e^{-i\phi} - l_- \sin^2\frac{\theta}{2} e^{i\phi} \right]. \end{aligned} \tag{6}$$

Note that $\theta = 0$ and $\phi = 0$ are taken at the c and a principal axes, respectively, of the original tetragonal lattice. By including this term with the second variational technique, we calculate the variation of the total energy by changing the magnetization direction with the force theorem.[35–39] Calculated spin easy axis is [110] for $PbVO_3$ and [001] for $BiCoO_3$, while hard axis is [001] for $PbVO_3$ and [100] for $BiCoO_3$. Relative values of MAE to the easy axis are listed in Table I. It is interesting to note that the magnitude of MAE in $BiCoO_3$ is much larger by a factor of five than that in $PbVO_3$ and its easy and hard axes are opposite to each other. In the case of $BiCoO_3$, the first-principles result on the easy axis is in good agreement with experiment.[19] Unfortunately, no experimental result is known for $PbVO_3$. We also evaluated spin and orbital magnetic moments in the muffin-tin sphere as listed in Table II. For each direction of the quantization axis, the orbital magnetic moment aligns antiferromagnetically

Table I. Calculated magnetic anisotropy energies of $PbVO_3$ and $BiCoO_3$ in meV/formula unit. Relative energies to the easy axis are shown. Directions [001] and [100] correspond to the z and x-axis, respectively, of the non-magnetic tetragonal lattice.

	[001]	[100]	[110]	[111]
$PbVO_3$	0.520	0.004	0	0.260
$BiCoO_3$	0	2.538	2.534	1.263

Table II. Calculated spin and orbital magnetic moments of the transition-metal site in $PbVO_3$ and $BiCoO_3$ for each easy axis in μ_B.

	orbital	spin
$PbVO_3$	-0.025	0.75
$BiCoO_3$	0.145	2.48

in $PbVO_3$ and ferromagnetically in $BiCoO_3$ to the spin magnetic one. The magnitude of the orbital moment in $BiCoO_3$ is greater than that in $PbVO_3$ by about six. This may be due to large spin moment and strong SOI in $BiCoO_3$ (see §5.3). We also evaluate the full θ and ϕ dependences of MAE and calculated results in the xz-plane ($\phi = 0$) and xy-plane ($\theta = \pi/2$) are shown in Fig. 1 for $PbVO_3$ and in Fig. 2 for $BiCoO_3$. For both cases, a $\cos 2\theta$ dependence is found in the xz-plane while a $\cos 4\phi$ dependence is obtained in the xy-plane with quite small magnitude compared with the θ-dependence. With the tetragonal lattice symmetry given, the $\cos 2\theta$ and $\cos 4\phi$ dependences are easily understood because of two-fold and four-hold rotation symmetry, respectively. We analyze the origin of the angle and material dependences in MAE with a perturbation theory in the following section.

5. Analysis with a Perturbation Theory

In the previous section, different MAE behaviors are seen between $PbVO_3$ and $BiCoO_3$. In addition, the angle dependence of MAE is found to be $\cos 2\theta$ in the xz-plane and $\cos 4\phi$ in the xy-plane for both oxides. As already pointed out, two oxides have similar electronic structure.[24] So the origin of these similarity and dissimilarity in the electronic and magnetic properties needs to be examined in detail. We now analyze the first-principles results of MAE with help of a perturbation theory. In evaluating the matrix elements of SOI with $l = 2$, it is convenient to rewrite spherical harmonics Y_{lm} with cubic harmonics defined as

$$d_{xy} = -\frac{i}{\sqrt{2}}\left(Y_{22} - Y_{2-2}\right), \tag{7}$$

$$d_{yz} = \frac{i}{\sqrt{2}}\left(Y_{21} + Y_{2-1}\right), \tag{8}$$

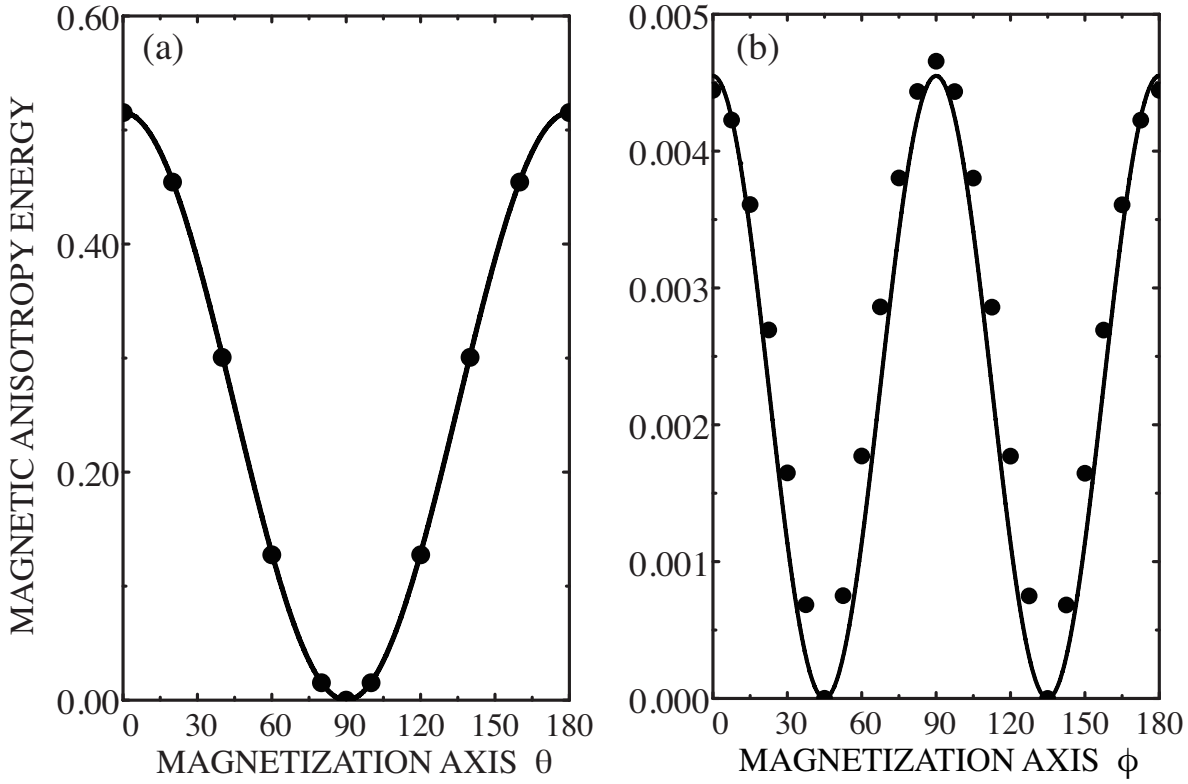

Fig. 1. Calculated magnetic anisotropy energy (MAE) of $PbVO_3$ in meV/formula unit. (a) On xz-plane ($\phi = 0$), MAE at $\theta = 90°$ is taken as the origin and dots and line show calculated points and a fitted curve to $\cos 2\theta$, respectively, as a function of magnetization axis θ in degree. (b) On xy-plane ($\theta = 90°$), MAE at $\phi = 45°$ is as the origin and dots and line denote calculated points and a fitted curve to $\cos 4\phi$, as a function of magnetization axis ϕ in degree.

$$d_{zx} = -\frac{1}{\sqrt{2}}\left(Y_{21} - Y_{2-1}\right), \tag{9}$$

$$d_{x^2-y^2} = \frac{1}{\sqrt{2}}\left(Y_{22} + Y_{2-2}\right), \tag{10}$$

$$d_{3z^2-r^2} = Y_{20}. \tag{11}$$

With these cubic harmonics and radial function $R_2(r)$, we easily evaluate the perturbation matrix element $\langle i, \sigma | H_{so}(\theta, \phi) | j, \sigma' \rangle$ $(i, j = xy, yz, zx, x^2 - y^2, 3z^2 - r^2)$ with respect to spin quantization axes θ and ϕ. Detailed methods to calculate the matrix elements follows the previous works.[47,48] The first-order change in wavefunctions is easy to evaluate from the similar procedure to MAE. In that case, the expectation value of the orbital magnetic moment $\langle l_\alpha \rangle$ parallel to the spin quantization axis α is obtained from the same matrix elements.[48]

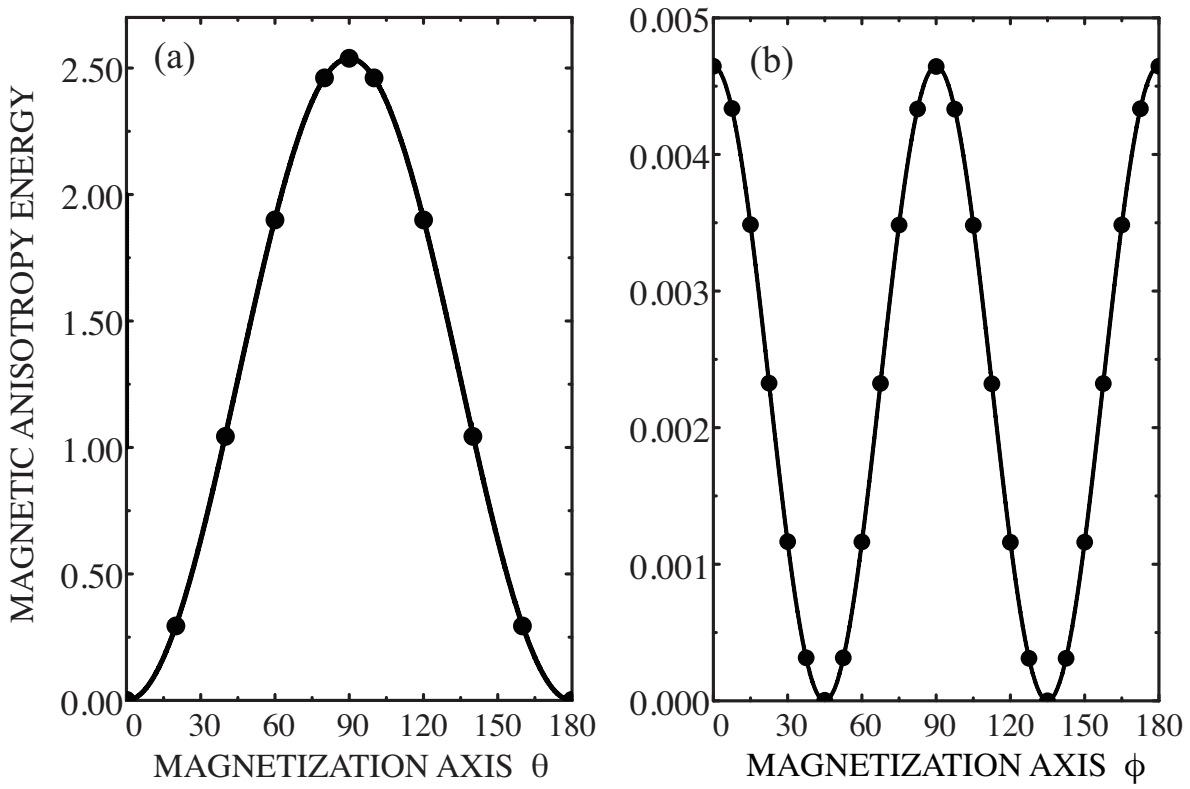

Fig. 2. Calculated magnetic anisotropy energy (MAE) of $BiCoO_3$ in meV/formula unit. (a) On xz-plane ($\phi = 0$), MAE at $\theta = 0°$ is taken at the origin and dots and line show calculated points and a fitted curve to $\cos 2\theta$, respectively, as a function of magnetization axis θ in degree. (b) On xy-plane ($\theta = 90°$), MAE at $\phi = 45°$ is at the origin and dots and line denote calculated points and a fitted curve to $\cos 4\phi$, respectively, as a function of magnetization axis ϕ in degree.

5.1 $PbVO_3$

In this section, we discuss MAE of $PbVO_3$. For the perturbation theory, we need to determine energy levels of V-3d state. From the DFT calculation, we simplify these energy levels, $E_{i\sigma}$ ($i = xy, yz, zx, x^2 - y^2, 3z^2 - r^2$ and $\sigma = \uparrow, \downarrow$), as shown in Fig. 3. The energy of each orbital is measured from that of the majority-spin xy level and is labeled by Δ_n ($n = 1, 2, 3$) as $\Delta_1 = E_{yz,zx\uparrow} - E_{xy\uparrow}$, $\Delta_2 = E_{xy\downarrow} - E_{xy\uparrow}$ and $\Delta_3 = E_{yz,zx\downarrow} - E_{xy\uparrow}$. Based on this schematic energy diagram, we evaluate the magnetic anisotropy energy with the first and second-order perturbation theory. On account of $\langle xy, \uparrow | H_{so} | xy, \uparrow \rangle = 0$, the first-order energy shift goes to zero. The second-order energy shift $\Delta E^{(2)}$ is evaluated by taking into account the unoccupied $d\epsilon$ states as the intermediated states of the second-order process. Noting that $\langle xy, \uparrow | H_{so} | xy, \downarrow \rangle = 0$, we have the leading second-order terms as

$$\Delta E^{(2)} = -\frac{\lambda_2^2}{2\Delta_1}\Big(1 - \cos 2\theta\Big) - \frac{\lambda_2^2}{2\Delta_3}\Big(3 + \cos 2\theta\Big), \tag{12}$$

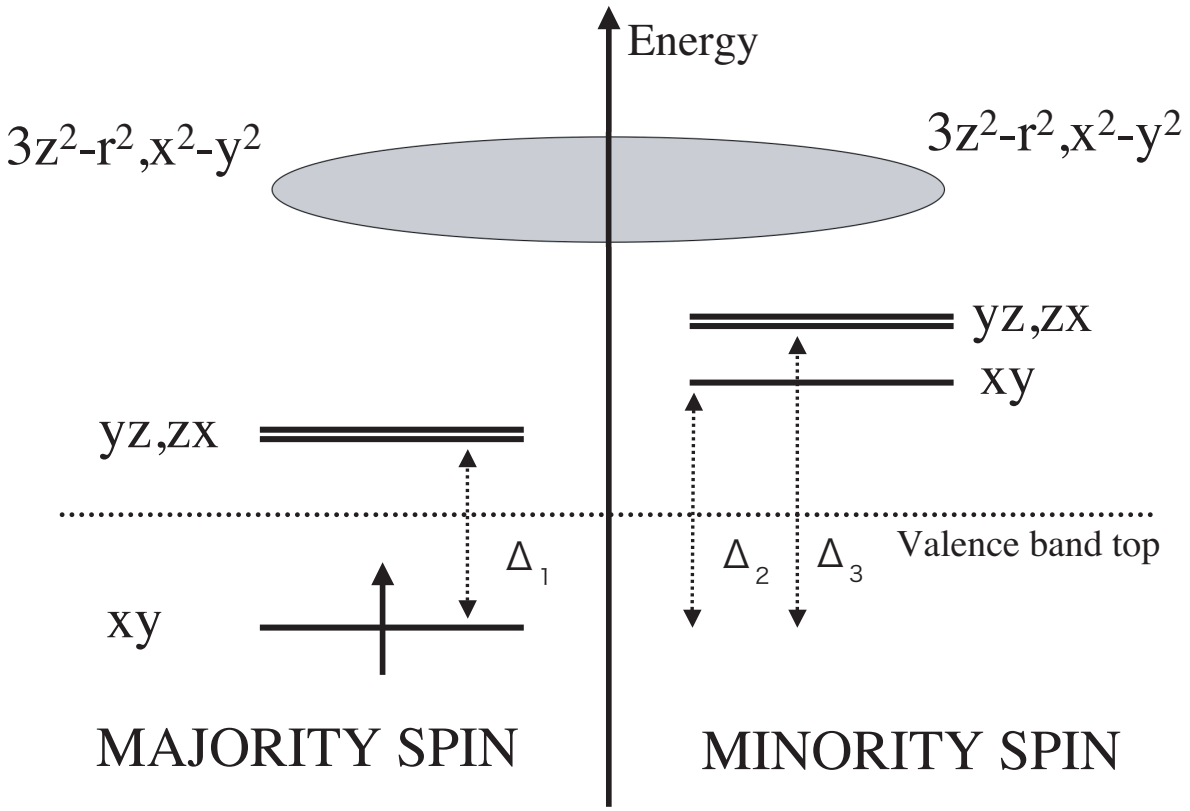

Fig. 3. Schematic energy diagram in $PbVO_3$. Only the xy orbital with majority spin is occupied with V^{4+} (d^1) configuration. The $3z^2 - r^2$ and $x^2 - y^2$ orbitals are located in high energy with large dispersion.

with SOI parameter λ_l given below (see §5.3). The angle dependent part of $\Delta E^{(2)}$ is called MAE as given by

$$E_{\mathrm{MAE}}(\theta, \phi) = \frac{\lambda_2^2}{2}\Big(\frac{1}{\Delta_1} - \frac{1}{\Delta_3}\Big)\cos 2\theta. \tag{13}$$

Equation (13) shows that the spin-preserve Δ_1 and spin-flip Δ_3 process have the opposite contributions to the leading terms of MAE. Due to $\Delta_1 < \Delta_3$ MAE has a $\cos 2\theta$ dependence with a positive sign, including that the magnetization easy axis resides on the xy plane. This accounts for the first-principles result shown in Fig. 1 (a). The ϕ dependence is clearly vanished in the perturbation theory up to second order. From the form of the spin-orbit operator shown in eq. (6), a $\cos 4\phi$ dependence will be obtained from the fourth-order perturbation with quite small magnitude. For the easy axis of [110] in $PbVO_3$ and we obtain the orbital magnetic moment as

$$\langle l_{110} \rangle = -\frac{2\lambda_2}{\Delta_1}. \tag{14}$$

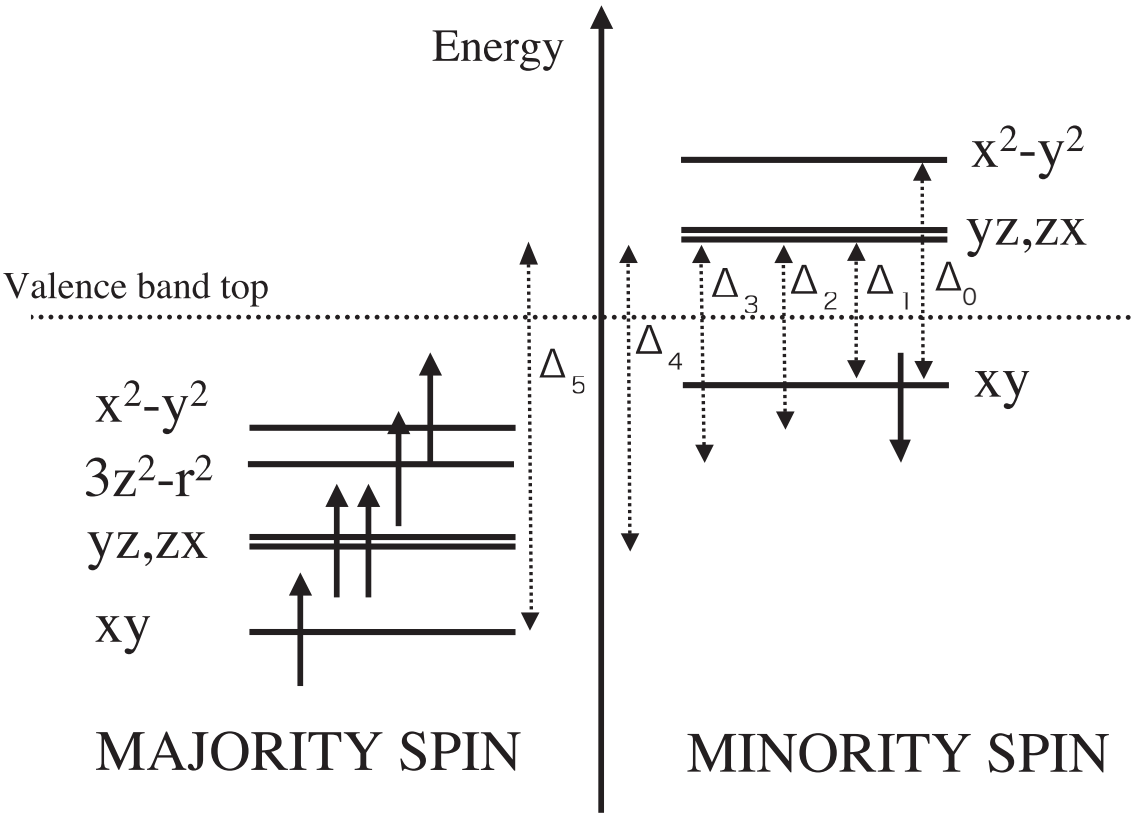

Fig. 4. Schematic energy diagram in $BiCoO_3$. All the majority-spin d bands and the xy band with the minority spin are occupied with Co^{3+} (d^6) configuration. Unoccupied $3z^2 - r^2$ band with the minority spin is located in a high energy region.

The sign is also consistent with the first-principles result. With inclusion of $3z^2 - r^2$ and $x^2 - y^2$ orbitals, no apparent qualitative change from the result is expected because of their large Δ.

5.2 $BiCoO_3$

As in $PbVO_3$, we assume simplified energy levels for $BiCoO_3$ as shown in Fig. 4, where each energy level is measured from that of the minority spin yz, zx level and is also labeled by Δ_n ($n = 1, 2, 3, 4, 5$) as Δ_n indicate $\Delta_1 = E_{yz,zx\downarrow} - E_{xy\downarrow}$, $\Delta_2 = E_{yz,zx\downarrow} - E_{x^2-y^2\uparrow}$, $\Delta_3 = E_{yz,zx\downarrow} - E_{3z^2-r^2\uparrow}$, $\Delta_4 = E_{yz,zx\downarrow} - E_{yz,zx\uparrow}$ and $\Delta_5 = E_{yz,zx\downarrow} - E_{xy\uparrow}$. In $Co^{3+}(d^6)$ case, the initial states are $|xy,\uparrow\rangle$, $|yz,\uparrow\rangle$, $|zx,\uparrow\rangle$, $|x^2-y^2,\uparrow\rangle$, $|3z^2-r^2,\uparrow\rangle$ and $|xy,\downarrow\rangle$ and the intermediate states are $|yz,\downarrow\rangle$, $|zx,\downarrow\rangle$. The $|x^2 - y^2,\downarrow\rangle$ and $|3z^2 - r^2,\downarrow\rangle$ states may be neglected. The first-order energy shift goes to be zero again. With these conditions, the second-order energy shift $\Delta E^{(2)}$ is given by

$$\Delta E^{(2)} = \lambda_2^2 \Big[A + B\cos 2\theta \Big], \tag{15}$$

where A and B are given by

$$A = -\frac{1}{2\Delta_1} - \frac{3}{2\Delta_2} - \frac{9}{2\Delta_3} - \frac{1}{\Delta_4} - \frac{3}{2\Delta_5}, \tag{16}$$

$$B = \frac{1}{2\Delta_1} - \frac{1}{2\Delta_2} - \frac{3}{2\Delta_3} + \frac{1}{\Delta_4} - \frac{1}{2\Delta_5}. \tag{17}$$

In this case, MAE becomes

$$E_{\mathrm{MAE}}(\theta, \phi) = \lambda_2^2 B \cos 2\theta, \tag{18}$$

The magnitude and sign of MAE are determined by the relative values of Δ. By inspecting the energy diagram in Fig. 4, Δ_4 and Δ_5 are large and their contributions are negligible, and Δ_3 and Δ_2 look almost the same. For simplicity, by putting $\Delta_2 \approx \Delta_3 \equiv \Delta_{eg}$ we have

$$E_{\mathrm{MAE}}(\theta, \phi) \approx \frac{\lambda_2^2}{2}\Big[\frac{1}{\Delta_1} - \frac{4}{\Delta_{eg}}\Big] \cos 2\theta. \tag{19}$$

Therefore, the leading term of MAE is represented by the competing two processes: a spin flip transition from the occupied e_g states to the unoccupied yz and zx states, and a spin diagonal transition from the minority xy to the yz and zx states. $\Delta_{eg} < 4\Delta_1$ is apparently satisfied from the energy diagram and MAE has a $\cos 2\theta$ dependence with a negative sign. In the same way as the previous $PbVO_3$ case, the ϕ dependence does not appear by the second-order perturbation and a $\cos 4\phi$ term will come from the fourth-order perturbation with small magnitude. These perturbation considerations are consistent with the first-principles result shown in Fig. 2. To evaluate the orbital magnetic moment properly, it is necessary to include the contribution from the minority-spin x^2-y^2 orbital. The resulting orbital magnetic moment is given as

$$\langle l_{001} \rangle = \frac{8\lambda_2}{\Delta_0}. \tag{20}$$

with $\Delta_0 = E_{x^2-y^2\downarrow} - E_{xy\downarrow}$. The sign of this term is also consistent with the first-principles one.

5.3 Comparison between $PbVO_3$ *and* $BiCoO_3$

From the perturbation theory with the first-principles energy diagram, we obtain the same angle dependence as the first-principles one. As mentioned before, both oxides have large tetragonal distortion and off-centering atomic displacement. Crystal field with largely distorted O_6 octahedron results in unconventional d-orbital energy splitting with low-lying xy orbital level. Under this electronic structure condition, MAE comes basically from the matrix elements between the occupied xy orbital and unoccupied (yz, zx) orbitals of V in the majority spin. In the case of Co, the occupied $(x^2 - y^2, 3z^2 - r^2)$ orbitals in majority spin and unoccupied (yz, zx) orbitals in the minority spin are involved in determining MAE. The ϕ dependences are clearly vanished in two cases from the second-order perturbation theory. A $\cos 4\phi$ dependence will come from the fourth-order perturbation and these magnitudes should

be quite small. These are consistent with our first-principles results.

Let us discuss the magnitude of anisotropy energy in the two cases. The magnitude of the θ dependent term is almost five times different between $PbVO_3$ and $BiCoO_3$. This is understood by the magnitude of SOI constant λ_l. In our implementation, λ_l can be evaluated with the radial functions as

$$\lambda_l = \int R_l^2(r)\lambda(r)r^2 dr. \tag{21}$$

Here R_l is the radial function defined inside the muffin-tin sphere. We neglect small spin dependence in λ_l. The λ_2 values for V-d in $PbVO_3$ is 17 meV and 45 meV for Co-d in $BiCoO_3$. The value in $BiCoO_3$ is about three times larger than that in $PbVO_3$. From λ_2 and Δ_n derived from first-principles calculations,[24] the amplitude of the angle dependence in xz-plane can be estimated to be 0.19 meV for $PbVO_3$ with Δ_1=0.5 eV and Δ_3=1.5 eV in eq. (13). In the case of $BiCoO_3$, we obtain the amplitude of 1.69 meV with Δ_1=1 eV and Δ_{eg}=1.5 eV in eq. (19). These results are in fairly good agreement with the first-principles results 0.26 meV for $PbVO_3$ and 1.27 meV for $BiCoO_3$ shown in Figs. 1 and 2. Therefore, the magnitude of SOI is one of the main reason to lead to the difference in MAE. The difference in the orbital magnetic moment also follows the tendency in MAE. As seen in first-principles result Table II and eqs. (14) and (20), the difference in the orbital moment comes from the energy-level distances and SOI.

These findings may suggest that applying pressure, stress or electric field can change the electronic structure via the lattice degree of freedom, leading to a possible cross correlation between ferroelectric or piezoelectric and magnetic anisotropy. In this connection, a noteworthy experimental approach to the cross correlation between the electric field and magnetic anisotropy in the metal-insulator-(magnetic)semiconductor structure has been quite recently reported.[49] A preliminary estimation of the correlation shows the variation of MAE due to the displacement of transition-metal ions to be $|\Delta E_{\rm MAE}/\Delta u_{\rm Co}| \sim 0.01$ eV/Å for $BiCoO_3$.

6. Conclusions

We have studied the magnetic anisotropy for multiferroic $PbVO_3$ and $BiCoO_3$ by using the first-principles calculations. As a result, the magnetic easy axes are [110] for $PbVO_3$ and [001] for $BiCoO_3$. The orbital magnetic moment of the transition-metal site in $BiCoO_3$ is greater than that in $PbVO_3$ by about six. The full θ and ϕ dependences of MAE are calculated. The θ dependence of MAE is given by $\cos 2\theta$, its sign is different between two oxide cases and its amplitude for $BiCoO_3$ is five times greater than that for $PbVO_3$. These differences are discussed with the perturbation theory using the energy diagram obtained from the first-principles calculations. It is found that the sign is determined by the spin diagonal $xy \rightarrow (yz, zx)$ transition in $PbVO_3$ and by the spin off-diagonal $(x^2-y^2, 3z^2-r^2) \rightarrow (yz, zx)$ one in $BiCoO_3$. The difference in the magnitude of MAE comes mainly from the magnitude

of SOI.

Acknowledgment

The authors are grateful to A. A. Belik, M. Azuma, Y. Shimakawa, S. Blügel, H. Funakubo, H. Naganuma and S. Yasui for fruitful discussions. One of the author Y. U. was supported by the Japan Society for the Promotion of Science. This work was partly supported by Grant-in-Aid for Scientific Research (No.19GS0207) from the Ministry of Education, Culture, Sports, Science and Technology of Japan. The computation in this work has been carried out using the facilities of the Supercomputer Center, Institute for Solid State Physics, University of Tokyo and Information Media Center, Hiroshima University.

References

1) G. A. Smolenskii and E. Chupis: Sov. Phys. JETP. **25** (1982) 475.
2) W. Prellier, M. P. Singh and P. Murugavel: J. Phys.: Condens. Matter **17** (2005) R803.
3) N. A. Spaldin and M. Fiebig: Science **309** (2005) 391.
4) T. Kimura, T. Goto, H Shintani, K. Ishizaka, T. Arima and Y. Tokura: Nature (London) **426** (2003) 55.
5) Y. Tokura and N. Nagaosa: Science **288** (2000) 462.
6) T. Atou, H. Chiba, K. Ohoyama, Y. Yamaguchi and Y. Shono: J. Solid State Chem. **145** (1999) 639.
7) N. A. Hill and K. M. Rabe: Phys. Rev. B **59** (1999) 8759.
8) A. Moreira dos Santos, A. K. Cheetham, T. Atou, Y. Syono, Y. Yamaguchi, K. Ohoyama and H. Chiba: Phys. Rev. B **66** (2002) 064425.
9) T. Kimura, S. Kawamoto, I. Yamada, M. Azuma, M. Takano and Y. Tokura: Phys. Rev. B **67** (2003) 180401(R).
10) C. Yang, S. Lee, T. Y. Koo and Y. H. Jeong: Phys. Rev. B **75** (2007) 140104.
11) E. Montanari, G. Calestani, L. Righi, E. Gilioli, F. Bolzoni, K. S. Knight and P. G. Radaelli: Phys. Rev. B **75** (2007) 220101(R).
12) T. Shishidou, N. Mikamo, Y. Uratani, F. Ishii and T. Oguchi: J. Phys.: Condens. Mater **16** (2004) S5677.
13) N. A. Hill: J. Phys. Chem. B **104** (2000) 6694.
14) P. Baettig, R. Seshadri and N. A. Spaldin: J. Am. Chem. Soc. **129** (2007) 32.
15) A. A. Belik, S. Iikubo, T. Yokosawa, K. Kodama, N. Igawa, S. Shamoto, M. Azuma, M. Takano, K. Kimoto, Y. Matsui and E. Tateyama-Muromachi: J. Am. Chem. Soc. **129** (2007) 971.
16) J. Wang, J. B. Neaton, H. Zheng, V. Nagarajan, S. B. Ogale, B. Liu, D. Viehland, V. Vaithyanathan, D. G. Schlom, U. V. Waghmare, N. A. Spaldin, K. M. Rabe, M. Wuttig and R. Ramesh: Science **299** (2003) 1719.
17) R. V. Shpanchenko, V. V. Chernaya, A. A. Tsirlin, P. S. Chizhov, D. E. Sklovsky and E. V. Antipov: Chem. Mater. **16** (2005) 3267.
18) A. A. Belik, M. Azuma, T. Saito, Y. Shimakawa and M. Takano: Chem. Mater. **17** (2005) 269.
19) A. A. Belik, S. Iikubo, K. Kodama, N. Igawa, S. Shamoto, S. Niitaka, M. Azuma, Y. Shimakawa, M. Takano, F. Izumi and E. Tateyama-Muromachi: Chem. Mater. **18** (2006) 798.
20) L. W. Martin, Q. Zhan, Y. Suzuki, R. Ramesh, M. Chi, N. Browning, T. Mizoguchi and J. Kreisel: Appl. Phys. Lett., **90** (2007) 062903.
21) M. Azuma, S. Niitaka, N. Hayashi, K. Oka, M. Takano, H. Funakubo and Y. Shimakawa: Jpn. J. Appl. Phys. **47** (2008) 7579.
22) S. Yasui, H. Naganuma, S. Okamura, K. Nishida, T. Yamamoto, T. Iijima, M. Azuma, H. Morioka, K. Saito, M. Ishikawa, T. Yamada and H. Funakubo: Jpn. J. Appl. Phys. **47** (2008) 7582.
23) K. Oka, I. Yamada, M. Azuma, S. Takeshita, K. H. Satoh, A. Koda, R. Kadono, M. Takano and Y. Shimakawa: Inorg. Chem. **47** (2008) 7355.
24) Y. Uratani, T. Shishidou, F. Ishii and T. Oguchi: Jpn. J. Appl. Phys. **44** (2005) 7130.
25) D. J. Singh: Phys. Rev. B **73** (2006) 094102.
26) M. Q. Cai, J. C. Liu, G. W. Yang, Y. L. Cao, X. Tan and X. Y. Chen Y. G. Wang L. L. Wang

and W. Y. Hu: J. Chem. Phys. **126** (2007) 154708.
27) P. Ravindran, R. Vidya, O. Eriksson and H. Fjellvåg: Adv. Mater. **20** (2007) 1353.
28) R. D. King-Smith and D. Vanderbilt: Phys. Rev. B **47** (1993) 1651(R).
29) W. Kohn and L. J. Sham: Phys. Rev. **140** (1965) A1133.
30) J. F. Janak, V. L. Moruzzi and A. R. Williams: Phys. Rev. B **12** (1975) 1257.
31) O. K. Andersen: Phys. Rev. B **12** (1975) 3060.
32) D. D. Koelling and G. O. Arbman: J. Phys. F **5** (1975) 2041.
33) M. Weinert: J. Math. Phys. **22** (1981) 2433.
34) E. Wimmer, H. Krakauer, M. Weinert and A. J. Freeman: Phys. Rev. B **24** (1981) 864.
35) D. D. Koelling and B. N. Harmon: J. Phys. C **10** (1977) 3107.
36) A. H. MacDonald, W. E. Pickett and D. D. Koelling: J. Phys. C **13** (1980) 2675.
37) A. R. Macintosh and O. K. Andersen: M. Springford, ed., *Electrons at the Fermi Surface.* (Cambridge University Press, 1980).
38) M. Weinert, R. E. Watson and J. W. Davenport: Phys. Rev. B **32** (1985) 2115.
39) A. I. Liechtenstein, K. I. Latsnelson, V. P. Antropov and V. A. Gubanov: J. Magn. Magn. Mater. **67** (1987) 65.
40) K. Iwashita, T. Oguchi and T. Jo: Phys. Rev. B **54** (1996) 1159.
41) T. Shishidou and T. Oguchi: Phys. Rev. B **62** (2000) 11747.
42) H. Miyazawa, E. Natori, S. Myyashita, T. Shimoda, F. Ishii and T. Oguchi: Jpn. J. Appl. Phys. **39** (2000) 5679.
43) F. Ishii and T. Oguchi: J. Phys. Soc. Jpn. **71** (2002) 336.
44) Y. Uratani, T. Shishidou, F. Ishii and T. Oguchi: Physica B. **383** (2006) 9.
45) Y. Uratani, T. Shishidou and T. Oguchi: Jpn. J. Appl. Phys. **47** (2008) 7735.
46) P. E. Blöchl, O. Jepsen and O. K. Andersen: Phys. Rev. B **49** (1994) 16223.
47) H. Takayama, K. Bohnen and P. Fulde: Phys. Rev. B **14** (1976) 2287.
48) P. Bruno: Phys. Rev. B **39** (1989) 865(R).
49) D. Chiba, M. Sawicki, Y. Nishitani, F. Matsukura, Y. Nakatani and H. Ohno: Nature(London) **455** (2008) 515.